

Article

Not peer-reviewed version

---

# Quantitative Proteomics Analysis of ABA and GA3 Treated Malbec Berries Reveals Insights into H<sub>2</sub>O<sub>2</sub> Scavenging and Anthocyanin Dynamics

---

[Germán Murcia](#)<sup>\*</sup>, [Rodrigo Alonso](#), [Federico Berli](#), Leonardo Arias, Luciana Bianchimano, Mariela Pontin, [Ariel Fontana](#), [Jorge José Casal](#), Patricia Piccoli

Posted Date: 12 August 2024

doi: 10.20944/preprints202408.0826.v1

Keywords: abscisic acid; gibberellic acid; grapevine; hydrogen peroxide; berry ripening; ROS



Preprints.org is a free multidiscipline platform providing preprint service that is dedicated to making early versions of research outputs permanently available and citable. Preprints posted at Preprints.org appear in Web of Science, Crossref, Google Scholar, Scilit, Europe PMC.

Copyright: This is an open access article distributed under the Creative Commons Attribution License which permits unrestricted use, distribution, and reproduction in any medium, provided the original work is properly cited.

Article

# Quantitative Proteomics Analysis of ABA and GA<sub>3</sub> Treated Malbec Berries Reveals Insights into H<sub>2</sub>O<sub>2</sub> Scavenging and Anthocyanin Dynamics

Germán Murcia <sup>1,\*†</sup>, Rodrigo Alonso <sup>2†</sup>, Federico Berli <sup>2</sup>, Leonardo Arias <sup>2</sup>,  
Luciana Bianchimano <sup>1</sup>, Mariela Pontin <sup>3</sup>, Ariel Fontana <sup>2</sup>, Jorge José Casal <sup>1,4</sup> and Patricia Piccoli <sup>2</sup>

<sup>1</sup> Fundación Instituto Leloir, Instituto de Investigaciones Bioquímicas de Buenos Aires, CONICET, Buenos Aires Argentina; lbianchimano@leloir.org.ar (L.B.); jcasal@leloir.org.ar (J.J.C.)

<sup>2</sup> Instituto de Biología Agrícola de Mendoza, CONICET-Universidad Nacional de Cuyo, Mendoza, Argentina; ralonso@fca.uncu.edu.ar (R.A.); fberli@fca.uncu.edu.ar (F.B.); laarias@mdp.edu.ar (L.A.); afontana@mendoza-conicet.gob.ar (A.F.); ppiccoli@fca.uncu.edu.ar (P.P.)

<sup>3</sup> INTA-EEA La Consulta, Mendoza, Argentina; pontin.mariela@inta.gob.ar (M.P.)

<sup>4</sup> Facultad de Agronomía, Universidad de Buenos Aires, CONICET, Instituto de Investigaciones Fisiológicas y Ecológicas Vinculadas a la Agricultura (IFEVA), Buenos Aires, Argentina

\* Correspondence: mmurcia@leloir.org.ar

† These authors have made equal contributions to this work and are considered joint first authors.

**Abstract:** Abscisic acid (ABA) and gibberellic acid (GA<sub>3</sub>) are regulators of fruit color and sugar levels, and the application of these hormones is a common practice in commercial vineyards dedicated to the production of table grapes. However, the effects of exogenous ABA and GA<sub>3</sub> on wine cultivars remains unclear. We investigated the impact of ABA and GA<sub>3</sub> applications on Malbec grapevine berries across three developmental stages. We found similar patterns of berry total anthocyanin accumulation, induced by both treatments, closely associated with berry H<sub>2</sub>O<sub>2</sub> levels. Quantitative proteomics revealed that ABA and GA<sub>3</sub> positively modulated antioxidant defense proteins, mitigating H<sub>2</sub>O<sub>2</sub>. Consequently, proteins involved in phenylpropanoid biosynthesis were downregulated, leading to decreased anthocyanin content at almost ripe stage, particularly petunidin-3-G and peonidin-3-G. Additionally, we noted increased levels of the non-anthocyanins E-viniferin and quercetin in the treated berries, which may enhance H<sub>2</sub>O<sub>2</sub> scavenging at almost ripe stage. Using a linear mixed-effects model, we found statistical significance of the fixed effects berry H<sub>2</sub>O<sub>2</sub> and sugar contents, demonstrating their roles in anthocyanin accumulation. In conclusion, our findings suggest a common molecular mechanism by which ABA and GA<sub>3</sub> influence berry H<sub>2</sub>O<sub>2</sub> content, ultimately impacting anthocyanin dynamics during ripening.

**Keywords:** abscisic acid; gibberellic acid; grapevine; hydrogen peroxide; berry ripening; ROS

## 1. Introduction

Grapevines stand as the most economically significant fruit crop worldwide. In Argentina, 92% of the grapevine cultivation area is dedicated to the wine industry, with Malbec being the predominant variety (www.inv.gob.ar). The development and ripening of grape berries involve complex physiological processes marked by dynamic changes in biochemical composition and color. Berry development follows a double sigmoid growth curve with three distinct phases, two periods of growth separated by a lag phase during which cell expansion slows and seeds mature [1]. At the end of the lag phase, a brief period known as *veraison* indicates the onset of ripening which is characterized by a rapid accumulation of sugar and anthocyanins in red grape varieties [1]. Polyphenols, particularly anthocyanins, in grape berry skins, play a pivotal role in determining red wine quality. In grapevines, polyphenols are classified into two primary groups: non-flavonoids (hydroxybenzoic and hydroxycinnamic acids and their derivatives, stilbenes, and phenolic alcohols)

and flavonoids (anthocyanins, flavanols and flavonols) [2]. Generally, they act as phytoalexins, photoprotectants and potent antioxidants, helping plants mitigate biotic and abiotic stresses [3]; and in grape berry skins, play pivotal role in determining sensory attributes and wine quality.

The hormones abscisic acid (ABA) and gibberellins (GAs) are key regulators of berry development and ripening [4]. In grape berries, classified as non-climacteric fruits, the concentration of ABA increases at *veraison*, influencing the timing of ripening [5], and then declines to low levels. The concomitant increase in ABA levels and berry sugars positively modulates the expression of genes involved in the phenylpropanoid pathway, stimulating downstream biosynthesis and accumulation of anthocyanins [6,7]. The application of ABA enhances sugar transport to the berries by promoting phloem area and up-regulating sugar transport genes, accelerates berry ripening and boosts anthocyanin levels in both wine and table grapes [5,8–12].

GAs, along with auxins and cytokinins, promote cell division and expansion during the initial stages of berry development. GAs levels in berry tissues are increased during the early stages and then decrease at the initiation of ripening. GAs are primarily synthesized by the seeds, and the final size of the berry depends on the number of seeds [1]. Consequently, the application of gibberellic acid ( $GA_3$ ) is commonly employed in seedless grapevine cultivars [13]. Moreover, GAs enhance the sink strength of seeded berries, playing a pivotal role in sugar accumulation [8,14]. However, whilst in the cultivar Malbec, the application of  $GA_3$  significantly delays the onset of berry ripening and reduces anthocyanin accumulation at *veraison* [8], in table grapes it increases polyphenol content in the berry skin [13].

Although, ABA and  $GA_3$  applications are widely used in table grapes to enhance berry color development and sugar accumulation, respectively, their commercial use in wine grapes remains limited by the lack of a comprehensive understanding concerning their effects [13,15–17].

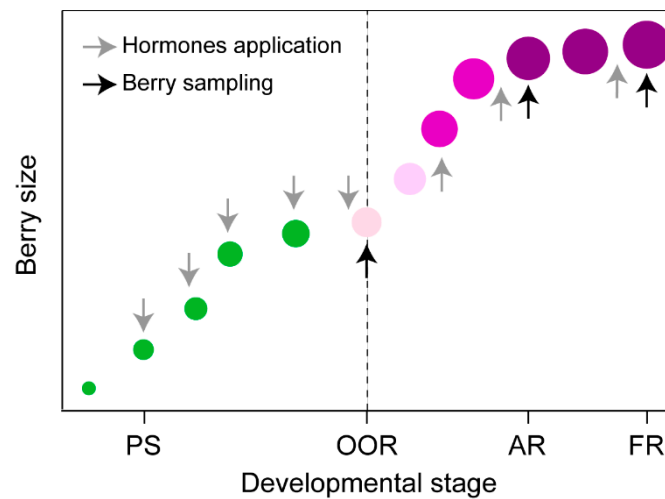
Fruit ripening requires the turnover of reactive oxygen species (ROS), including free radicals such as hydroxyl radicals ( $\cdot OH$ ) and superoxide anions ( $O_2^{\cdot -}$ ), and molecules such as hydrogen peroxide ( $H_2O_2$ ) and singlet oxygen ( $^1O_2$ ) [18–20]. In plants, ROS are generated during basal metabolism across various organelles, including mitochondria (aerobic respiration), chloroplasts (photosynthesis), and peroxisomes (photorespiration) [21]. Additionally, several cell wall- and plasma membrane-localized enzymes contribute to ROS production, such as NADPH oxidases, amine oxidases, quinone reductases, lipoxygenases, class III peroxidases, and oxalate oxidases [22]. ROS are neutralized by plant's antioxidative defense mechanisms, which include both enzymatic and non-enzymatic systems. Enzymatic defense involves superoxide dismutase (SOD), catalase (CAT), ascorbate peroxidase (APX), and glutathione peroxidase (GPX), while non-enzymatic defense relies on antioxidants like proline, glutathione, ascorbic acid, carotenoids and flavonoids [23,24]. Elevated ROS levels exceeding scavenging capacities induce oxidative stress, causing cellular damage and potential death. Conversely, at low levels, ROS function as second messengers in growth, development, and stress responses [25]. The onset of fruit ripening in both climacteric and non-climacteric fruits (grape berries) correlates with  $H_2O_2$  accumulation and modulation of ROS scavenging enzymes, suggesting ROS involvement in fruit development [26–30]. Applications of  $H_2O_2$  to Kyoho grape berries hastening the accumulation of anthocyanins and Total Soluble Solids (TSS), followed by up-regulation of genes associated with oxidative stress, cell wall deacetylation and cell wall degradation [31,32]. There is also evidence of an interplay between ROS and phytohormones like ABA promoting berry ripening [33], even at a molecular level [34]. However, the link between ABA/ $GA_3$  and ROS in the regulation of fruit ripening remains largely unexplored.

In this study, we applied exogenous ABA and  $GA_3$  to the aerial parts of Malbec grapevines to evaluate their effects on berry ripening and anthocyanin dynamics on it. Physiological, biochemical and proteomics approaches were used in this study to demonstrate the hypothesis that ABA and  $GA_3$  modulate  $H_2O_2$  levels in berries, consequently influencing berry ripening (anthocyanins and TSS accumulation). We found significant differences regarding berry total anthocyanins dynamics among ABA and  $GA_3$  treatments due to differences on TSS and  $H_2O_2$  contents. Moreover, ABA and  $GA_3$  positively modulated antioxidant defense proteins, reducing berry  $H_2O_2$  levels at almost ripe developmental stage.

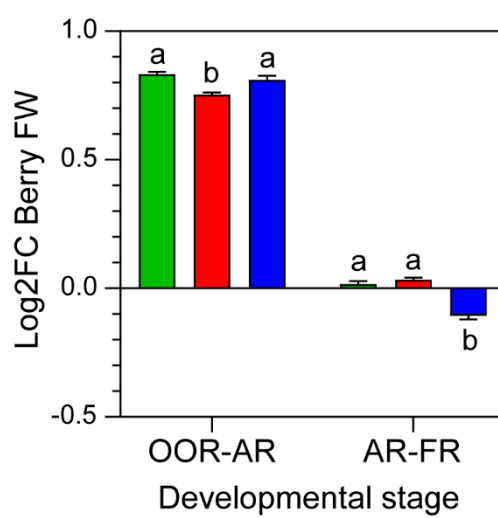
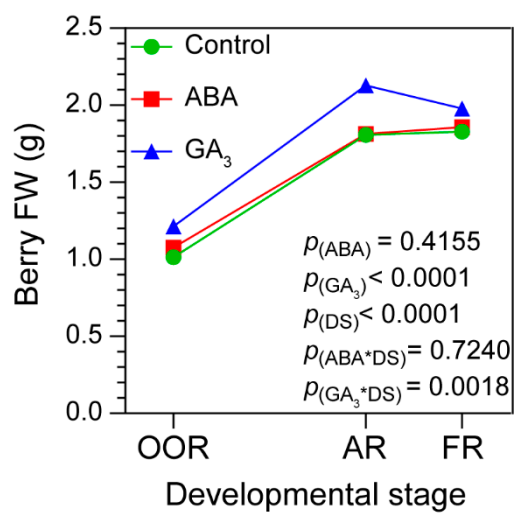
## 2. Results

### 2.1. GA<sub>3</sub> Promotes BFW and TSS Accumulation during Berry Ripening, Whilst ABA Has No Effect

The impact of ABA and GA<sub>3</sub> applications on Malbec grapevine berries across three developmental stages was investigated (Figure 1A). The GA<sub>3</sub> treatment increased the overall BFW (berry fresh weight) during the different berry ripening stages, with no significant differences observed between the control and ABA treatments (Figure 1B). ABA-treated berries showed the lowest BFW Log<sub>2</sub> Fold-Change (Log<sub>2</sub>FC) from OOR (onset of ripening developmental stage) to AR (almost ripe developmental stage), and GA<sub>3</sub>-treated berries denoted the lowest BFW fold change from AR to FR (full ripening developmental stage, Figure 1C). The TSS on a per berry basis increased continuously until FR (Figure 1D), and GA<sub>3</sub> treatment promoted it regardless of the berry ripening stages, while no differences were observed between the control and ABA treatments (Figure 1D). When Log<sub>2</sub>FC TSS was compared among developmental stages, it was observed that ABA- and GA<sub>3</sub>-treated berries significantly reduced TSS accumulation from OOR to AR (Figure 1E). Finally, ABA and GA<sub>3</sub> treatments showed no differences on TSS accumulation from AR to FR, compared to the control (Figure 1E).

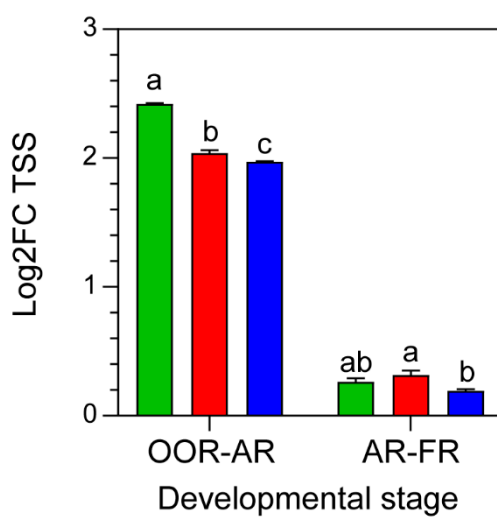
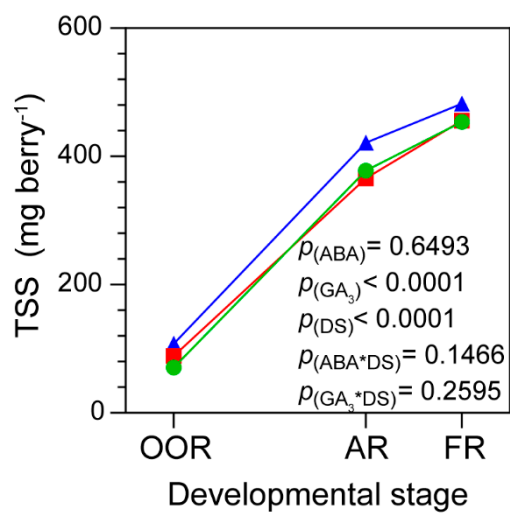


(A)



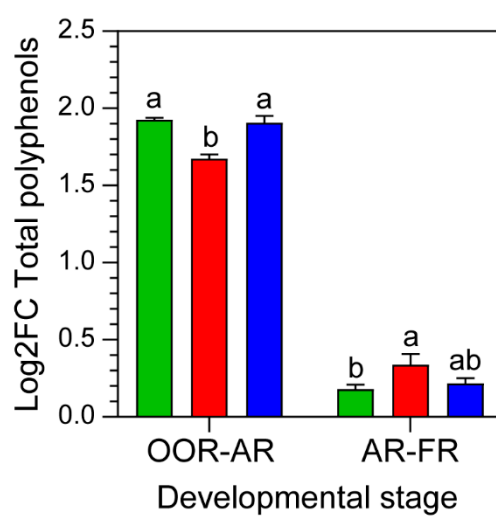
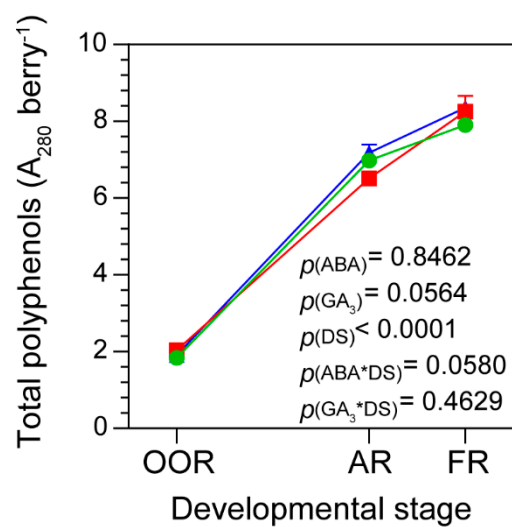
(B)

(C)



(D)

(E)



(F)

(G)

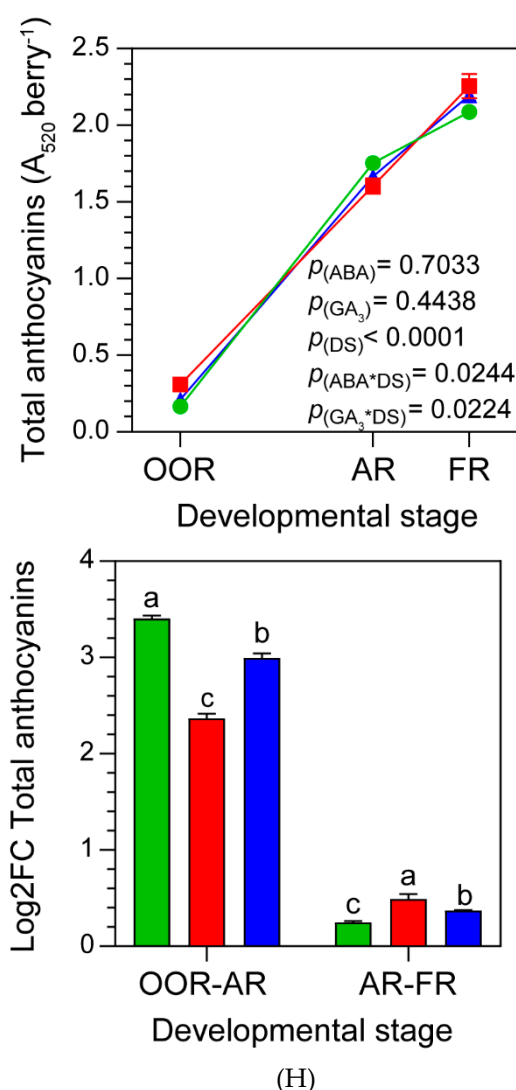


**Figure 1.** (A) Scheme of hormones applications and berry sampling during berry growth and development. Hormones were applied every two weeks starting at PS. PS: berry pea-size stage, OOR: onset of ripening stage, AR: almost ripe stage and FR: full ripening stage. Vertical dashed line indicates *veraison* stage. (B) Berry Fresh Weight; (D) Total Soluble Solids per berry; (F) total polyphenols per berry; (H) total anthocyanins per berry according to developmental stage and treatment. (C, E, G, I) Log<sub>2</sub> Fold Change of each variable from OOR to AR (OOR-AR), and from AR to FR (AR-FR). Values are means  $\pm$  SE,  $n=3$ . Some errors can not be shown because SE are smaller than the symbol.  $p_{(ABA)}$ ,  $p_{(GA_3)}$  and  $p_{(DS)}$ : effects of ABA,  $GA_3$  and developmental stage, respectively;  $p_{(ABA*DS)}$  and  $p_{(GA_3*DS)}$ : interaction effects of factors. One- and two-way ANOVA followed by Fisher's LSD test were applied. Different letters indicate significant differences ( $p < 0.05$ ).

## 2.2. ABA and $GA_3$ Modify the Phenolic Compounds Dynamics during Berry Ripening

Berry total polyphenols and anthocyanins increased from OOR to FR (Figure 1F,H). ABA-treated berries accumulated the fewest total polyphenols from OOR to AR, and significantly increased the accumulation from AR to FR (Figure 1G). In addition, control berries showed the lowest accumulation of total polyphenols from AR to FR (Figure 1G). In relation to total anthocyanins, ABA applications likely anticipated the onset of ripening due to the higher content of anthocyanins at OOR. Moreover, ABA treatment showed statistically less berry total anthocyanins at AR and a tendency to increase the berry total anthocyanins at FR, compared to the control (ABA\*DS significant interaction, Figure 1H). In line with this, ABA applications decreased berry total anthocyanins accumulation rate (Log<sub>2</sub>FC) from OOR to AR and increased it from AR to FR (Figure 1I). A similar pattern was observed with  $GA_3$  treatment, where the accumulation of berry total anthocyanins was

significantly less from OOR to AR and higher from AR to FR, compared to the control (Figure 1I). In this case, GA<sub>3</sub> decreased the berry total anthocyanins content (significant GA<sub>3</sub>\*DS interaction) at AR, compared to the control (Figure 1H).

### 2.3. ABA and GA<sub>3</sub> Promote a Shift in Polyphenols Metabolism at AR

Figure 2A showed all the polyphenols detected in berries at AR. ABA treatment decreased the content of the anthocyanins petunidin-3-G, peonidin-3-G and delphinidin-3-acet and increased the levels of the non-anthocyanins E-viniferin, ferulic acid, myricetin, OH-tyrosol, astilbin and quercetin. Moreover, ABA decreased the berry total anthocyanins content, showing no effects on berry total non-anthocyanins and polyphenols, compared to the control (Figure 2B, C and D). GA<sub>3</sub> decreased the anthocyanins petunidin-3-G, peonidin-3-G, and the non-anthocyanins OH-tyrosol, astilbin, ferulic acid and myricetin, and only increased the non-anthocyanins E-viniferin and quercetin, compared to the control (Figure 2A). In addition, GA<sub>3</sub> treatment had no effect on berry total anthocyanins and polyphenols (Figure 2A and C, respectively), whilst it increased the content of berry total non-anthocyanins, compared to the control (Figure 2B). Interestingly, both ABA and GA<sub>3</sub> treatments changed the polyphenols metabolism, promoting the accumulation of non-anthocyanins in detriment of anthocyanins at AR (Figure 2E).

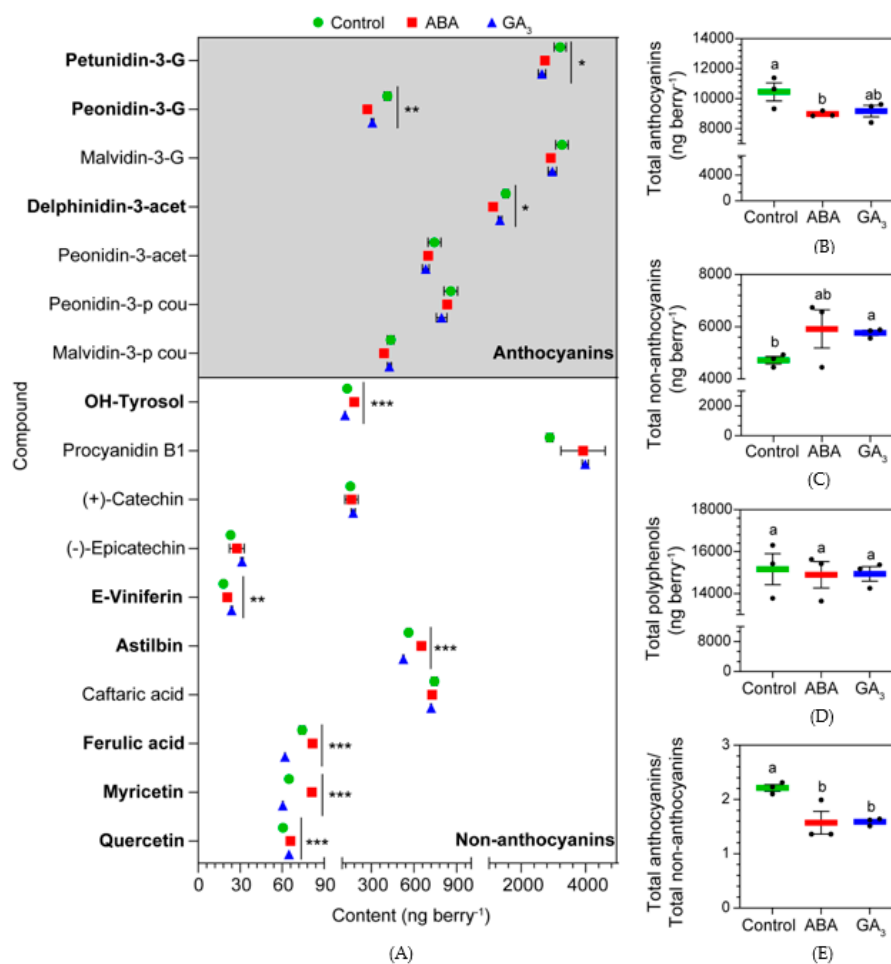


**Figure 2.** (A) Anthocyanins and non-anthocyanins (low mass weight polyphenols) found in berries at almost ripe stage (AR); (B) total anthocyanins per berry at AR; (C) total non-anthocyanins per berry at AR; (D) total polyphenols per berry at AR; (E) total anthocyanins/total non-anthocyanins ratio per berry at AR. Values are means  $\pm$  SE,  $n=3$ . Some errors can not be shown because SE are smaller than the symbol. One-way ANOVA followed by Fisher's LSD test was applied. Different letters indicate significant differences ( $p < 0.05$ ). Significance codes: (\*\*\*)  $p < 0.001$ , (\*\*)  $p < 0.01$ , (\*)  $p < 0.05$ . G: glucoside, acet: acetylglucoside, p cou: p-coumaroylglucoside.

#### 2.4. ABA and GA<sub>3</sub> Modify Berry H<sub>2</sub>O<sub>2</sub> Content Dynamics during Berry Ripening

Figure 3A showed that ABA-treated berries had high berry H<sub>2</sub>O<sub>2</sub> contents at OOR and markedly reduced berry H<sub>2</sub>O<sub>2</sub> levels at AR (ABA\*DS significant interaction). This pattern was similar for GA<sub>3</sub>-treated berries. In this sense, GA<sub>3</sub> applications significantly increased the berry H<sub>2</sub>O<sub>2</sub> content at OOR to then significantly decreased it at AR (GA<sub>3</sub>\*DS significant interaction). No statistical differences were found in berry H<sub>2</sub>O<sub>2</sub> content at FR neither with ABA nor GA<sub>3</sub>, compared to the control. In addition, opposite to the control, a degradation of berry H<sub>2</sub>O<sub>2</sub> either with ABA or GA<sub>3</sub> applications from OOR to AR was found (Figure 3B). On the contrary, these hormones induced the accumulation of berry H<sub>2</sub>O<sub>2</sub> from AR to FR, compared to the control (Figure 3B).

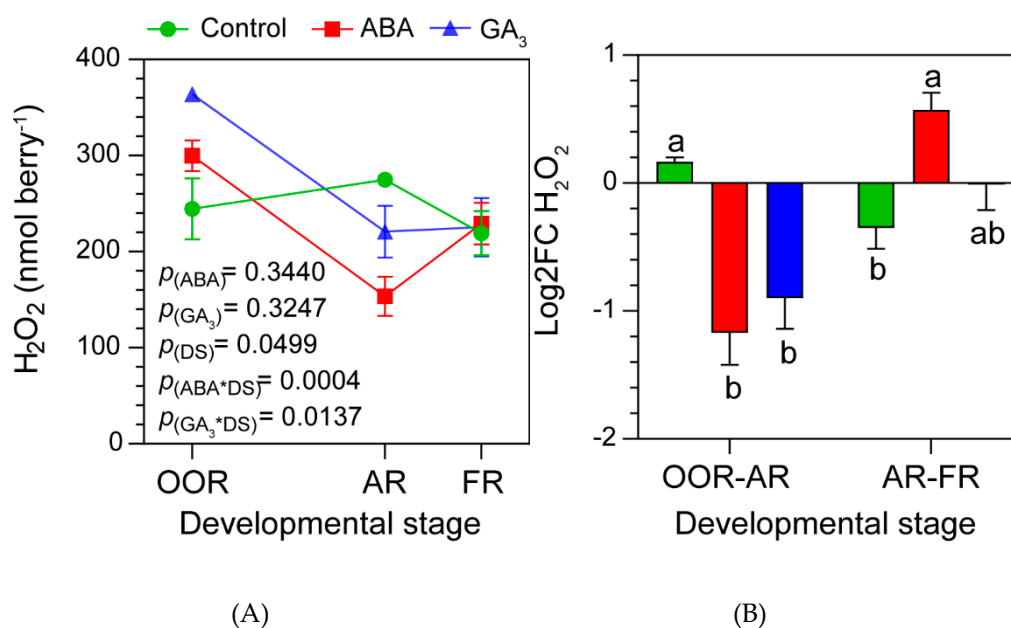


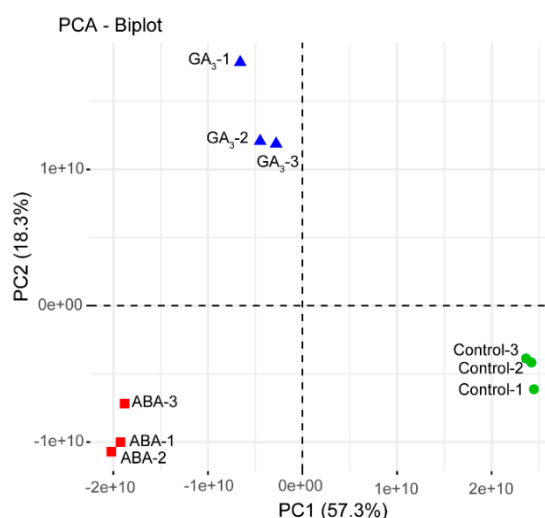
**Figure 3.** (A) Hydrogen peroxide (H<sub>2</sub>O<sub>2</sub>) content in berries according to developmental stage and treatment. Values are means  $\pm$  SE,  $n=3$ . Some errors can not be shown because SE are smaller than the symbol.  $p_{(ABA)}$ ,  $p_{(GA_3)}$  and  $p_{(DS)}$ : effects of ABA, GA<sub>3</sub> and developmental stage, respectively;  $p_{(ABA*DS)}$  and  $p_{(GA_3*DS)}$ : interaction effects of factors. (B) Log<sub>2</sub> Fold Change of H<sub>2</sub>O<sub>2</sub> from OOR to AR (OOR-AR), and from AR to FR (AR-FR). One- and two-way ANOVA followed by Fisher's LSD test were applied. Different letters indicate significant differences ( $p < 0.05$ ).

#### 2.5. ABA and GA<sub>3</sub> Positively Modulate the Enzymatic Antioxidant Defense System

##### 2.5.1. ABA and GA<sub>3</sub> Differentially Modulate the Berry Skin Proteome

A total of 1638 proteins were identified and quantified at AR, of which 685 were differentially abundant proteins (DAPs) using a cutoff  $q$ -value of  $<0.05$  (Supplementary Table S1). Principal Component Analysis (PCA) of the 1638 proteins confirmed the uniformity of the biological replicates as the three groups of replicates clustered tightly (Figure 4A). The greatest variance in protein abundance was found between control and GA<sub>3</sub>- and ABA-treated samples, as they were separated along the first component (57.3% of the total variance). In particular, the largest difference was evident between the control and the ABA-treated berries. On the other hand, the second principal component (18.3% of the total variance) separated efficiently the ABA-treated berries from the GA<sub>3</sub>-treated ones. The 685 DAPs were used as input queries to perform a k-means clustering heatmap analysis. The most representative GO terms were assigned to each cluster to better visualize the main function of each treatment (Figure 4B). Interestingly, it was found that cluster 1 (96 up-regulated proteins co-expressed by ABA and GA<sub>3</sub>) grouped most of the proteins into response to H<sub>2</sub>O<sub>2</sub> (GO: 0042542) and protein glutathionylation (GO: 0010731) categories (Figure 4B and Supplementary Figure S1A). Both GOs are related to mechanisms of oxidative stress alleviation. On the other hand, it was observed that cluster 4 (186 proteins up-regulated only in the control berries) grouped the

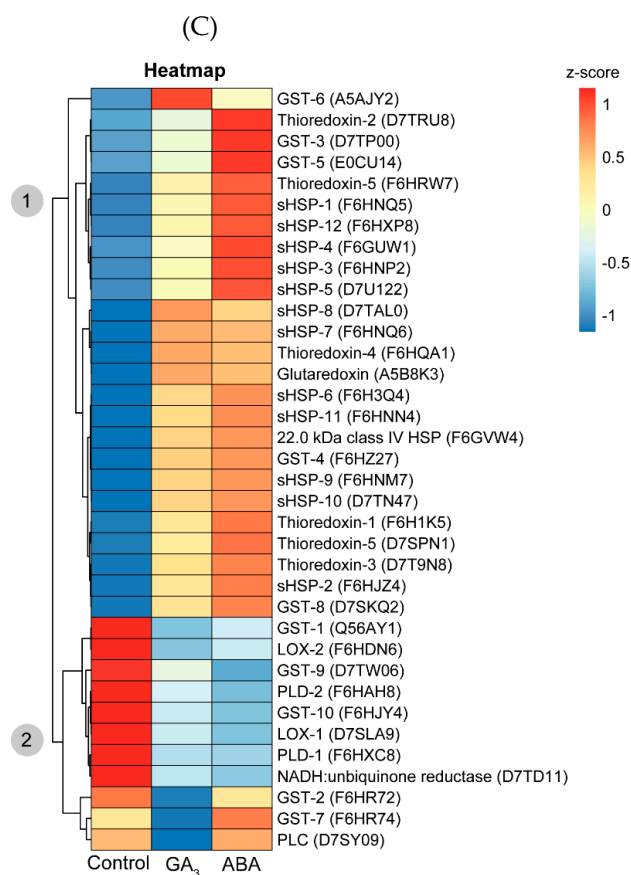
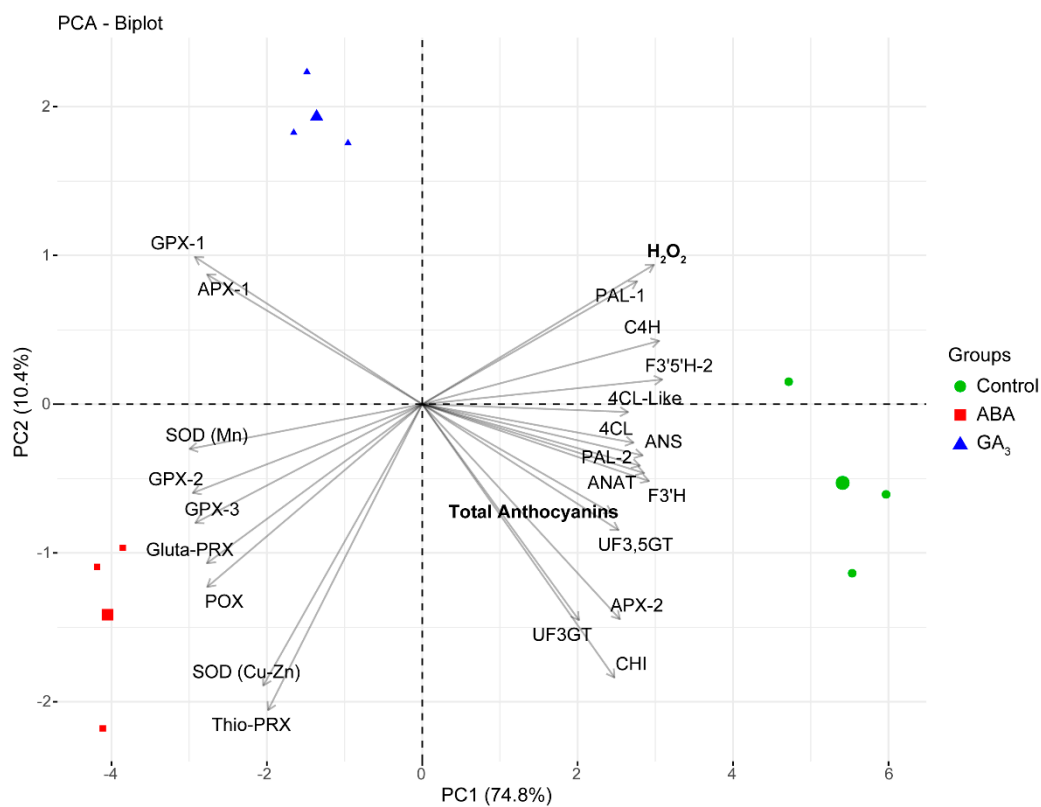
proteins into translation (GO: 0006412) and flavonoid biosynthetic pathway (GO: 0009813; Figure 4B and Supplementary Figure S1B). Different functional categories were specifically modulated by ABA and GA<sub>3</sub> treatments. ABA-treated berries mainly up-regulated the proteins sorted into proteasomal protein catabolic process (GO: 0010498) and photosynthesis (GO: 0015979) categories (cluster 5, size: 159 proteins, Figure 4B). As expected, this hormone also increased the abundance of proteins related to stress response suggested by the categories: response to reactive oxygen species (GO: 0000302), response to water deprivation (GO: 0009414), response to heat (GO: 0009408), response to oxidative stress (GO: 0006979), response to temperature stimulus (GO: 0009266), response to toxic substance (GO: 0009636) and detoxification (GO: 0098754) (Supplementary Figure S1C). In the case of GA<sub>3</sub>-treated berries, an overrepresentation of the categories: tricarboxylic acid metabolism (GO: 0072350) and oxidative photosynthetic carbon pathway (GO: 0009854) was observed (Figure 4B). In addition, this hormone up-regulated the proteins related to the aromatic and L-serine and L-glycine amino acids metabolism suggested by the categories: L-phenylalanine biosynthetic process (GO: 0009094), aromatic amino acid family biosynthetic process (GO: 0009073), glycine biosynthetic process from serine (GO: 0019264), glycine metabolic process (GO: 0006544), L-serine catabolic process (GO: 0006565), serine family amino acid catabolic process (GO: 0009071), L-serine metabolic process (GO: 0006563), serine family amino acid metabolic process (GO: 0009069) and serine family amino acid biosynthetic process (GO: 0009070) (Supplementary Figure S1D).



(A)



(B)



(D)

**Figure 4.** (A) Principal component analysis (PCA) of the 9 protein abundance datasets at almost ripe stage (AR). Samples are sharply separated between control and treated samples (first principal

component) and between ABA- and GA<sub>3</sub>-treated berries (second principal component). (B) k-means clustering heatmap of the 685 differentially abundant proteins (DAPs) in control, ABA- and GA<sub>3</sub>-treated berry skins at AR. Size: corresponds to the number of proteins grouped in each cluster. GO: corresponds to the most representative gene ontology terms for biological processes of each cluster retrieved by STRING enrichment with a redundancy cutoff of 0. (C) PCA of variables measured at AR in control, ABA and GA<sub>3</sub>-treated berry skins. POX: Peroxidase domain-containing protein (E0CRP4), GPX-1: Glutathione peroxidase-1 (F6HUD1), GPX-2: Glutathione peroxidase-2 (F6H344), GPX-3: Glutathione peroxidase-3 (A5AU08), APX-1: L-ascorbate peroxidase-1 (F6H0K6), APX-2: L-ascorbate peroxidase-1 (F6I106), SOD (Mn): Superoxide dismutase (Mn) (F6HC76), SOD (Cu-Zn): Superoxide dismutase (Cu-Zn) (D7SNA2), Gluta-PRX: Glutaredoxin-dependent peroxiredoxin (D7TBK8), Thio-PRX: Thioredoxin-dependent peroxiredoxin (D7TH54), PAL-1: phenylalanine ammonia lyase-1 (F6HNF5), PAL-2: phenylalanine ammonia lyase-2 (A5BPT8), C4H: trans-cinnamate 4-monooxygenase (A5BRL4), 4CL: 4-coumarate-CoA ligase (F6GXF5), 4CL-Like: 4-coumarate-CoA ligase-Like (F6GW98), CHI: chalcone-flavonone isomerase (F6HC36), F3'H: flavonoid 3'-monooxygenase (D7SI22), F3'5'H-2: flavonoid 3',5'-hydroxylase-2 (F6HA82), ANS: anthocyanidin synthase (A2ICC9), UF3GT: UDP-glucose flavonoid 3-O-glucosyltransferase (D7SQ45), UF3,5GT: UDP-glucose: anthocyanidin 5,3-O-glucosyltransferase (A5BFH4) and ANAT: anthocyanin acyltransferase (D7TU67). (D) Heatmap of the oxidative stress response, reactive oxygen species (ROS) production and membrane degradation proteins in control, ABA- and GA<sub>3</sub>-treated berry skins at AR. The values > 0 in the heatmap images indicate up-regulated, while the values < 0 indicate down-regulated.

### 2.5.2. ABA and GA<sub>3</sub> Up-Regulate the Proteins with Antioxidant Function

ABA and GA<sub>3</sub> up-regulated, to a similar extent, the proteins that alleviate oxidative stress, and down-regulated those related to flavonoid biosynthetic pathway (Figure 4B). Figure 4C shows a PCA biplot mixing the data of DAPs corresponding to antioxidant and anthocyanins biosynthetic pathway enzymes, with the berry total anthocyanin and H<sub>2</sub>O<sub>2</sub> levels at AR. The PC1 explained 74.8% of the variability, and PC2 explained 10.4% of the variability. Regarding antioxidant enzymes, ten enzymes differentially abundant were found: one peroxidase domain-containing protein (POX), two L-ascorbate peroxidase (APX-1 and APX-2), three glutathione peroxidases (GPX-1, GPX-2 and GPX-3), two superoxide dismutases (SOD Mn and SOD Cu-Zn) and two peroxiredoxins (glutaredoxin-dependent peroxiredoxin, Gluta-PRX, and thioredoxine-dependent peroxiredoxin, Thio-PRX) (Supplementary Table S1). In relation to anthocyanins biosynthetic pathway enzymes, we found twelve enzymes differentially abundant: phenylalanine ammonia lyase-1 and two (PAL-1 and PAL-2), trans-cinnamate 4-monooxygenase (C4H), 4-coumarate-CoA ligase (4CL), 4-coumarate-CoA ligase-Like (4CL-Like), chalcone-flavonone isomerase (CHI), flavonoid 3'-monooxygenase (F3'H), flavonoid 3',5'-hydroxylase-2 (F3'5'H-2), anthocyanidin synthase (ANS or LDOX), UDP-glucose flavonoid 3-O-glucosyltransferase (UF3GT), UDP-glucose: anthocyanidin 5,3-O-glucosyltransferase (UF3,5GT) and anthocyanin acyltransferase (ANAT) (Supplementary Table S1 and Supplementary Figure S2).

Figure 4C shows that, all the antioxidant enzymes except for APX-2 were associated with ABA and GA<sub>3</sub> treatments, and all enzymes belonging to anthocyanins biosynthetic pathway were associated with the control. The enzymes GPX-1 and APX-1 were more closely associated with GA<sub>3</sub>-treated berries, meanwhile the remaining antioxidant enzymes were more closely associated with ABA-treated berries. Moreover, in control berries it was observed a clear association with total anthocyanins and H<sub>2</sub>O<sub>2</sub> levels.

### 2.5.3. ABA and GA<sub>3</sub> Up-Regulate the Oxidative Stress Response Proteins

A more detailed analysis of oxidative stress-related proteins was performed in the 685 DAPs (Supplementary Table S1). We found thirteen small heat shock proteins (sHSP-1 to 12 and 22 KDa class IV HSP), five thioredoxins (thioredoxin-1 to 5), one glutaredoxin and ten glutathion S-transferases (GST-1 to 10). We also found enzymes related to ROS production and membrane degradation caused by oxidative stress: one NADH:ubiquinone reductase, two lipoxygenases (LOX-

1 and LOX-2), two phospholipases D (PLD-1 and PLD-2) and one phospholipase C (PLC). Comparing their abundances among treatments by a heatmap, we observed two main clusters (Figure 4D). Cluster 1 grouped all the proteins up-regulated by ABA and GA<sub>3</sub> (Figure 4D). In this case, we found almost (except for 5 GSTs) all the proteins associated to oxidative stress response and alleviation (sHSP-1 to 12, 22 KDa class IV HSP, thioredoxin-1 to five and thioredoxin dependent peroxiredoxin, glutaredoxin, glutaredoxin-dependent peroxiredoxin, GST-3, GST-4, GST-5, GST-6 and GST-8) (Figure 4D). Contrary, cluster 2 grouped all the proteins up-regulated almost exclusively by the control (Figure 4D). In which, we found all the enzymes related to ROS production (NADH:ubiquinone reductase, LOX-1, LOX-2), membrane degradation (LOX-1, LOX-2, PLD-1, PLD-2 and PLC) and 5 GSTs (GST-1, GST-2, GST-7, GST-9 and GST-10). Finally, noting that the enzymes involved in membrane peroxidation were up-regulated in the control berries, we decided to assess the content of MDA, a product of lipid peroxidation. Contrary to the expected due to the upregulation of enzymes involved in membrane peroxidation, control berries presented significantly less MDA content than the hormone treatments (Supplementary Figure S3).

### 2.6. Berry Total Anthocyanins Accumulation Depends on Berry Sugar and H<sub>2</sub>O<sub>2</sub> Content

A linear mixed-effects model showed that the fixed effects "TSS" and "H<sub>2</sub>O<sub>2</sub>" were statistically significant with high predictive accuracy by the entire model ( $R^2=0.98$  and  $p<0.0001$ ) (Supplementary Table S2 and Figure 5). In addition, the total fixed effects explained 95% of the variance, out of a total of 98% explained by the model including both fixed and random effects (Supplementary Table S2). In this sense, the random effect "Treatment" only explained 3% of the variance (Supplementary Table S2). This result demonstrated that berry total anthocyanins accumulation positively depended on berry sugar and H<sub>2</sub>O<sub>2</sub> contents.

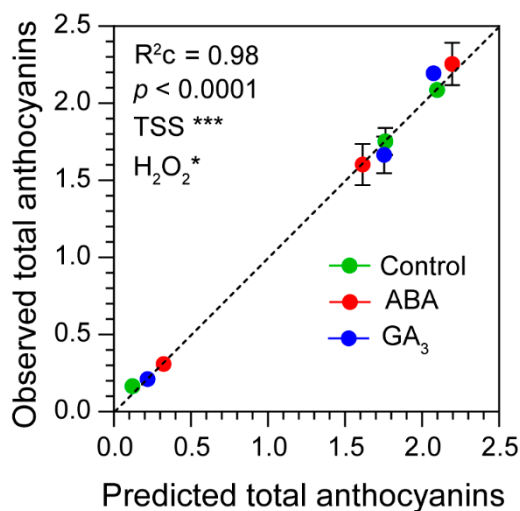


**Figure 5.** Observed total anthocyanins vs predicted total anthocyanins. Linear mixed-effects model using as fixed effects: TSS, Total Soluble Solids (g berry<sup>-1</sup>) and H<sub>2</sub>O<sub>2</sub>, hydrogen peroxide (nmol berry<sup>-1</sup>) and as random effect: Treatment (control, ABA and GA<sub>3</sub>). R<sup>2</sup>c, conditional R<sup>2</sup>, represents the variance explained by the entire model. Significance codes: (\*\*\*)  $p < 0.001$ , (\*\*)  $p < 0.01$ , (\*)  $p < 0.05$ .

### 3. Discussion

Our results show significant variations in H<sub>2</sub>O<sub>2</sub> levels during the ripening stages and to ABA and GA<sub>3</sub> treatments, subsequently impacting the dynamics of total anthocyanin accumulation throughout berry development. Importantly, the observed differences among treatments were attributed to the effects of TSS and H<sub>2</sub>O<sub>2</sub> ( $R^2=0.98$ ). Thus, berry total anthocyanins positively depended on berry sugar and H<sub>2</sub>O<sub>2</sub> contents. Both hormone treatments reduced berry H<sub>2</sub>O<sub>2</sub> content at AR, and this was associated with an increased abundance of proteins related to the antioxidant enzyme system. Finally, this reduction in berry H<sub>2</sub>O<sub>2</sub> levels was correlated with a downregulation of

the abundance of enzymes belonging to the anthocyanin biosynthesis pathway observed in the hormone treatments.

GA<sub>3</sub> is widely recognized in the table grapes industry for its role enhancing both yield and sugar content, especially in seedless berries [13], but is also effective in seeded wine grapes [8,14]. The present study provides additional evidence of GA<sub>3</sub>'s impact on berry physiology, increasing sugar accumulation on a per berry basis and berry growth during ripening, possibly as an enhancer of sink strength [8]. Interestingly, proteomic analysis unveiled the GA<sub>3</sub>-induced upregulation of two proteins associated with cell wall softening and fruit ripening as pectin esterase (F6HJZ5) and pectin acetyltransferase (D7TFE6; [35,36]). However, GA<sub>3</sub> treatment downregulated two expansins, expansin (E0CQY0) and expansin-B2 (D7SLR0), which are also linked to berry ripening, suggesting a complex mechanism regulating the berry growth by GA<sub>3</sub>.

The role of ABA in promoting the accumulation of anthocyanins in grape berries is well-established, primarily through the upregulation of structural and regulatory genes and the abundance of proteins associated with the phenylpropanoid biosynthesis pathway [37–40]. In the present study, ABA-treated berries exhibited a significant increase in anthocyanin content at OOR, highlighting the role of ABA as a major regulator of grape berry at early stages of ripening [5,10]. As berry maturity progressed, ABA treatment showed statistically less berry total anthocyanins at AR and a tendency to increase the berry total anthocyanins at FR. This dynamic variation between ABA-treated and control berries paralleled differences in H<sub>2</sub>O<sub>2</sub> dynamics during berry ripening. Thus, we demonstrated that ABA treatment modulated the synthesis and degradation of H<sub>2</sub>O<sub>2</sub>, thereby influencing the overall accumulation of berry total anthocyanins during ripening. These results are consistent with those indicating that ABA regulates ROS generation and accumulation by modulating the activity of NADPH oxidase, the primary enzyme catalyzing ROS generation in the apoplast, and inducing the degradation of H<sub>2</sub>O<sub>2</sub> through the upregulation of the *OsCATB* gene which encodes for the antioxidant enzyme catalase B in rice leaves [41–43].

Similar to that observed for ABA treatment, GA<sub>3</sub> applications significantly reduced total anthocyanins at AR, followed by an increase in their accumulation at FR stage. Again, these results were correlated with fluctuations in H<sub>2</sub>O<sub>2</sub> levels during berry ripening, with lower levels of H<sub>2</sub>O<sub>2</sub> at AR and higher accumulation of it from AR to FR. Previous studies have demonstrated the role of GA<sub>3</sub> in promoting antioxidant enzyme activities to maintain redox homeostasis under various environmental stresses [44]; however, our study represents the first report on the capability of GA<sub>3</sub> to induce ROS generation. Unlike ABA treatment, the presence of high levels of H<sub>2</sub>O<sub>2</sub> at OOR failed to promote a significant increase in total anthocyanin content in GA<sub>3</sub>-treated berries, a result that will be discussed in detail later in this section.

Gambetta et al. 2010 [6] demonstrated that grapevine orthologs of key sugar and ABA-signaling components are intricately regulated by the interplay between sugar and ABA, affecting the accumulation of total anthocyanins. They specifically evaluated Cabernet Sauvignon berries in two experimental systems: field-grown (deficit-irrigated) and cultured with sucrose and ABA. They found that the expression of the *VvMYBA1* gene, a crucial transcription factor responsible for activating anthocyanin biosynthesis, was significantly upregulated by sugars in the presence of ABA. Furthermore, Hung et al. 2008 [45] demonstrated that using a chemical trap for H<sub>2</sub>O<sub>2</sub>, dimethylthiourea, inhibits ABA-induced accumulation of anthocyanins in rice leaves. Additional evidence suggests that applications of ABA or H<sub>2</sub>O<sub>2</sub> to grapevine berries can accelerate the onset of ripening by upregulating the expression of phenylpropanoid biosynthesis pathway genes [32,39]. These findings collectively suggest that H<sub>2</sub>O<sub>2</sub> acts downstream of ABA signaling, with both H<sub>2</sub>O<sub>2</sub> and sugars acting as major regulators of total anthocyanin synthesis and accumulation. Consistent with these reports, our study revealed a dependence of berry total anthocyanin content during ripening on TSS and H<sub>2</sub>O<sub>2</sub> levels ( $R^2= 0.98$ ). ABA-treated berries at OOR exhibited higher total anthocyanin levels compared to the control, attributed to elevated H<sub>2</sub>O<sub>2</sub> content per berry basis. Then, ABA applications resulted in lower berry total anthocyanins accumulation from OOR to AR, corresponding to reduced TSS and H<sub>2</sub>O<sub>2</sub> accumulation relative to the control. Lastly, a significant increase in berry total anthocyanins accumulation was observed from AR to FR with ABA

applications, which correlated with increased H<sub>2</sub>O<sub>2</sub> accumulation compared to the control. Meanwhile, GA<sub>3</sub> treatment, despite inducing the highest levels of H<sub>2</sub>O<sub>2</sub> and TSS per berry basis at OOR, did not result in higher berry total anthocyanin content compared to ABA and control treatments, a pattern also evident at FR. These observations agree with previous studies by Loreti et al. 2008 [46], which demonstrated that sucrose-induced activation of the anthocyanin synthesis pathway was repressed by GA in Arabidopsis seedlings. In addition, recent findings by An et al. 2024 [47] suggest that GA may act as a repressor of anthocyanin synthesis by promoting the transcription and stability of MdbHLH162, which negatively regulates anthocyanin biosynthesis by disrupting the formation of anthocyanin-activated MdMYB1-MdbHLH3/33 complexes in apple. According to this, it is possible that GA<sub>3</sub> is acting as a repressor of anthocyanins synthesis in Malbec berry skins.

Observing the reduction in berry H<sub>2</sub>O<sub>2</sub> and total anthocyanins levels following ABA and GA<sub>3</sub> treatments at AR stage, a proteomic analysis was conducted to unravel a shared molecular mechanism governing this effect in grape berries. Both ABA and GA<sub>3</sub> upregulated proteins associated with the antioxidant enzymatic system, possibly alleviating H<sub>2</sub>O<sub>2</sub> levels. Specifically, increased abundances of ROS-scavenging enzymes: POX, SOD, GPX, APX and peroxiredoxins in response to both treatments were observed. This aligns with previous studies by which exogenous applications with ABA or GA<sub>3</sub> across various plant species, including grapevine [48,49], rice [43], maize [50,51] increased ROS scavenging enzymes activities under abiotic stresses. Furthermore, GA<sub>3</sub> treatments increased the activities of the antioxidant enzymes POX and SOD in *Phellodendron chinensis* seedlings growing at optimal conditions [52]. However, the modulation of H<sub>2</sub>O<sub>2</sub> levels by the enzymatic system in grapevine berries or other fruits regarding these hormones remains unexplored in existing literature. Our analysis further revealed that ABA treatment led to an augmentation in proteins associated with the GO term Photosynthesis (GO:0015979), particularly those related to photosystem II and ATP synthesis in the chloroplast: Oxygen-evolving enhancer protein 1 (F6I229), Oxygen-evolving enhancer protein 3-2 (F6H8B4), Chlorophyll a-b binding protein (F6HKS7), 23 kDa subunit of oxygen evolving system of photosystem II (A5B1D3), PsbP C-terminal domain-containing protein (E0CQM8), Photosystem II stability/assembly factor (D7T9G8), Ferredoxin (F6HK77) and ATP synthase delta chain (F6HVW3). This suggests that the sustained functioning of the thylakoid electron transport chain from H<sub>2</sub>O to NADP<sup>+</sup> reduces the likelihood of ROS generation. Accordingly, this could be one of the reasons for the differences observed between ABA and GA<sub>3</sub> regarding H<sub>2</sub>O<sub>2</sub> content at AR. ABA and GA<sub>3</sub> treatments induced an increase in proteins abundance linked to oxidative stress responses, including small heat shock proteins (sHSPs), thioredoxins and glutaredoxin, known for their multifaceted roles in mitigating oxidative stress [53–55]. Moreover, both treatments increased the protein abundance of five glutathione S-transferases (GSTs), known for their involvement in detoxification processes and in the attenuation of oxidative stress [56]. However, three GSTs (GST-1, GST-9 and GST-10) exhibited higher protein abundance in the control treatment, possibly indicating their role in anthocyanin transport from the endoplasmic reticulum to the vacuoles, as suggested by Sun et al. 2016 [57], given the higher accumulation of anthocyanins observed in this treatment at AR. Regarding ROS generation, in our proteomic dataset we could not identify and quantify the major enzyme that catalyzes the production of H<sub>2</sub>O<sub>2</sub> in the apoplast: NADPH oxidase. Instead, our attention was focused on NADH:ubiquinone reductase, a protein believed to be a significant source of ROS within mitochondria, contributing substantially to cellular oxidative stress [22,58]. Furthermore, our analysis revealed the presence of two lipoxygenases, LOX-1 and LOX-2, implicated in catalyzing membrane lipid peroxidation and subsequent liberation of H<sub>2</sub>O<sub>2</sub> from the enzyme surface, being potential ROS-generating enzymes [22,59]. Given the upregulation of NADH:ubiquinone reductase, LOX-1, and LOX-2 in control berry skins, we suggested that the increased activity of these enzymes accounted for the elevated H<sub>2</sub>O<sub>2</sub> levels observed at AR in this treatment. Considering the increased protein abundance of LOX-1, LOX-2, and two phospholipases D (PLD-1 and PLD-2), higher levels of MDA, a well-known indicator of membrane peroxidation might be expected. However, our hormonal treatments increased MDA content at AR compared to the control, suggesting that H<sub>2</sub>O<sub>2</sub> may serve primarily as a signaling

molecule rather than a toxic byproduct, thereby avoiding damage to cellular membranes, as suggested by Xi et al. 2017 [50].

In summary, berries treated with ABA and GA<sub>3</sub> exhibited reduced levels of H<sub>2</sub>O<sub>2</sub> at AR, attributed to the upregulation of ROS-scavenging proteins and the downregulation of ROS-generating proteins. Both treatments decreased anthocyanin content at AR, particularly petunidin-3-G and peonidin-3-G, correlated with a downregulation of the abundance of enzymes belonging to the anthocyanin biosynthesis pathway. However, both ABA and GA<sub>3</sub> treatments increased the protein abundance of the transcription factor Abscisic acid stress-ripening protein 2 (ASR2: F6GY46) at AR. ASR mediates glucose-ABA and glucose-GA crosstalk, modulating sugar accumulation and fruit ripening [61,62]. Accordingly, the up-regulation of ASR2 may have enhanced berry total anthocyanins accumulation from AR to FR observed in the ABA- and GA<sub>3</sub>-treated berries. ABA and GA<sub>3</sub> treatments prompted a metabolic shift from anthocyanin to non-anthocyanin biosynthesis at AR. In this sense, both ABA and GA<sub>3</sub> treatments led to increased levels of the stilbene E-viniferin and the flavonol quercetin compared to the control. Interestingly, these molecules exhibit potent antioxidant properties, surpassing even those of resveratrol [63]. Furthermore, it has been demonstrated that the specialized structure of quercetin, free 3-OH group and 3',4'-catechol, gives it the antioxidant property, which further helps in quenching off the ROS species generated by cells (reviewed in Singh et al. 2021 [64]). Consequently, the accumulation of E-viniferin and quercetin may boost ROS scavenging, thereby reducing the H<sub>2</sub>O<sub>2</sub> content at AR observed in ABA- and GA<sub>3</sub>-treated berries.

## 4. Materials and Methods

### 4.1. Plant Material and Experimental Conditions

The experiment was carried out during the 2016-2017 growing season in a commercial vineyard (La Pirámide, Catena Zapata winery; 33°09'58"S, 68°54'31"W and 1000 m asl, Mendoza, Argentina). Grapevines of a selected clone of *Vitis vinifera* L. cv. Malbec planted on their own roots were used. The vines were trained on a vertical trellis system arranged in north-south-oriented rows (2 m row spacing and 1.20 m between plants) and were maintained without soil water restriction using a drip irrigation system. The vines were cane-pruned and shoot-thinned to 12 shoots per vine and two clusters per shoot. The assay was set in a random design with three treatments (control, ABA and GA<sub>3</sub>) and three biological replicates. The biological replicate consisted of 5 plants from 7 consecutive plants in the row. Each biological replicate was sampled at onset of ripening (OOR, stage 35), almost ripe (AR, stage 37) and full ripening (FR, stage 38), based on Coombe et al. [65] (Figure 1A). ABA, GA<sub>3</sub> and water (control) solutions were sprayed with a hand-held sprayer onto the aerial parts of the plant (leaves and bunches) until runoff, with a 14 days frequency from berry pea-size stage (stage 31, Figure 1A) and during late afternoon to minimize ABA photodegradation. Treatment doses were: 1 mM ABA ( $\pm$ -S-cis, trans abscisic acid, PROTONE SL, Valent BioSciences, Libertyville, IL, USA), 1 mM GA<sub>3</sub> (GIBERELINA KA, S. Ando & Cía. SA, Buenos Aires, Argentina) and water (control). All solutions were supplemented with 0.05% (v/v) Triton X-100 as surfactant.

### 4.2. Berry Sampling, Fresh Weight and Total Soluble Solids

At each developmental stage (OOR, AR and FR), two days after the hormone application, 60 berries per biological replicate were randomly collected from 10 clusters (6 berries from each cluster: two top, two middle, and two bottom berries). The berries were placed in nylon bags and kept on dry ice to prevent protein degradation and dehydration. In the laboratory, 32 berries from each biological replicate were separated to perform berry fresh weight (BFW, g berry<sup>-1</sup>) and total soluble solids (TSS, °Brix). To do this, 32 berries were put into nylon bags and crushed by hand pressing, and the TSS was measured in the juice with a Pocket PAL-1 digital hand-held refractometer (Atago Co., Ltd., Tokyo, Japan). Then, the °Brix was multiplied by the BFW to express TSS in sugar on a per berry basis (mg berry<sup>-1</sup>). The remaining 28 berries from each biological replicate were stored at -80°C for further analysis.

#### 4.3. Berry Phenolic Extraction, Berry Total Polyphenols and Anthocyanins

Fifteen berries per biological replicate were deseeded and ground to a fine powder in liquid nitrogen using a mortar and pestle. One gram of the powder was then macerated with 10 mL of 1% HCl-methanol solution. The extraction was performed heating the samples at 70°C during 1 h, followed by three rounds of 5 min sonication in darkness. Then, the samples were centrifuged 10 min at 5000 g and the supernatant was collected for spectrophotometric measurements and chromatographic analysis. Absorbance of the extracts was read at 280 or 520 nm for determinations of total polyphenols and total anthocyanins, respectively, according to Berli et al. 2008 [66], with a Cary-50 UV-Vis spectrophotometer (Varian Inc., Palo Alto, CA, USA). Finally, the results were expressed on a per berry basis.

#### 4.4. Berry Phenolic Compounds Profile

Anthocyanins and non-anthocyanins (low molecular weight polyphenols, LMWP) were analyzed by high performance liquid chromatography with diode array and fluorescence detection (HPLC-DAD-FLD, Dionex Ultimate 3000 system, Dionex Softron GmbH, Thermo Fisher Scientific Inc., Germering, Germany). Anthocyanin determination was performed at AR according to Urvieta et al. 2018 [67] with minor adjustments. Briefly, a 500  $\mu$ L aliquot of berry phenolic extract (described for spectrophotometric measurements) was dried by vacuum centrifugation and dissolved in 1 mL of initial mobile phase prior to chromatographic analysis. Anthocyanins were separated in a reversed-phase Kinetex C18 column (3.0 $\times$ 100 mm, 2.6  $\mu$ m) Phenomenex (Torrance, CA, USA). The mobile phase was composed of ultrapure H<sub>2</sub>O:FA (formic acid):MeCN (acetonitrile) (87:10:3 v/v/v; eluent A) and ultrapure H<sub>2</sub>O:FA:MeCN (40:10:50 v/v/v; eluent B). Separation gradient was: 0 min, 10% B; 0-10 min, 25% B; 10-15 min, 31% B; 15-20 min, 40% B; 20-30 min, 50% B; 30-35 min, 100% B; 35-40 min, 10% B; 40-47 min, 10% B. Mobile phase flow, column temperature and injection volume were 1 mL min<sup>-1</sup>, 25°C and 5  $\mu$ L, respectively. Quantification was carried out by measuring peak area at 520 nm and the content of each anthocyanin was expressed as malvidin-3-glucoside equivalents, using an external standard calibration curve (1–250 mg L<sup>-1</sup>, R<sup>2</sup>=0.997). The identity of detected anthocyanins was confirmed by comparison with the elution profile and identification of analytes performed in previous research [68]. Then, the results were expressed on a per berry basis. For LMWP compounds, berry phenolic extracts were analyzed according to analytical conditions reported by Ferreyra et al. 2021 [69], using the same column as for anthocyanins. The mobile phase was an aqueous solution of 0.1% FA (solvent A) and MeCN (solvent B). The gradient was as follows: 0–1.7 min, 5% B; 1.7–10 min, 30% B; 10–13.5 min, 95% B; 13.5–15 min, 95% B; 15–16 min, 5% B; 16–19, 5% B. The total flow rate was set at 0.8 mL min<sup>-1</sup>. The column temperature was 35°C and the injection volume was 5  $\mu$ L. The identification of LMWP was based on the comparison of the retention times of phenolic compounds in samples with those of authentic standards. Standards of (+)-catechin ( $\geq$ 99%), (-)-epicatechin ( $\geq$ 95%), (+)-procyanidin B1 ( $\geq$ 90%), procyanidin B2 ( $\geq$ 90%), (-)-epigallocatechin ( $\geq$ 95%), (-)-gallocatechin gallate ( $\geq$ 98%), (-)-epicatechin gallate ( $\geq$ 95%), polydatin ( $\geq$ 95%), piceatannol ( $\geq$ 95%), (+)-E-viniferin ( $\geq$ 95%), quercetin hydrate (95%), quercetin 3- $\beta$ -d-galactoside ( $\geq$ 97%), quercetin 3- $\beta$ -d-glucoside ( $\geq$ 90%), kaempferol-3-glucoside ( $\geq$ 99%), myricetin ( $\geq$ 96%), naringin ( $\geq$ 95%), 3-hydroxytyrosol ( $\geq$ 99.5%), caftaric acid ( $\geq$ 97%), ferulic acid ( $\geq$ 99%), gallic acid (99%), phlorizdin ( $\geq$ 99%) were purchased from Sigma-Aldrich (St Louis, MO, USA). External calibration was used as a quantification approach. Linear ranges between 0.05 and 40 mg L<sup>-1</sup> with coefficient of determination (R<sup>2</sup>) higher than 0.993 were obtained. The results were expressed on a per berry basis. HPLC-grade MeCN and FA were sourced from Mallinckrodt Baker Inc. (Phillipsburg, NJ, USA). Ultrapure water was procured from a Milli-Q system (Millipore, Billerica, MA, USA).

#### 4.5. Berry Hydrogen Peroxide Content and Lipid Peroxidation

Measurements were done according to Junglee et al. 2014 [70], with some modifications. Briefly, 150 mg of deseeded berry frozen powder were homogenized with 1 ml of trichloroacetic acid (TCA; Sigma-Aldrich Corp., St Louis, MO, USA) buffer [0.25 ml TCA 0.1% (w/v), 0.5 ml KI 1 M, and 0.25 ml

K phosphate buffer 10 mM pH 8]) at 4°C for 10 min. The homogenate was centrifuged 15 min at 12000 g at 4°C. The supernatant was collected and incubated for 20 min at room temperature. Absorbance of the extracts was read at 350 nm with a Cary-50 UV-Vis spectrophotometer. A calibration curve obtained with H<sub>2</sub>O<sub>2</sub> standard solutions (100 vol., 30%) prepared in TCA buffer was used for quantification (8-100 nmol of H<sub>2</sub>O<sub>2</sub>, R<sup>2</sup>=0.999). Then, the results were expressed on a per berry basis.

Malondialdehyde (MDA) content was measured following the procedure described by Beligni and Lamattina 2002 [71]. For that, 100 mg of deseeded berry frozen powder were suspended in 2 mL of stock solution [15%, w/v TCA, 0.5%, w/v thiobarbituric acid (TBA, Sigma-Aldrich Corp., St Louis, MO, USA), and 0.25%, w/v hydrochloric acid (37%)]. The mixture was stirred vigorously and incubated at 95°C for 60 min. The samples were centrifuged at 9300 g for 10 min, the supernatant was collected, and the absorbance of the extracts was measured at 535 nm. The concentration was calculated considering MDA molar extinction coefficient =  $1.56 \times 10^5 \text{ M}^{-1} \text{ cm}^{-1}$ .

#### 4.6. Proteomic Analysis Using High-Resolution Mass Spectrometry

##### 4.6.1. Berry Skin Protein Extraction and Quantification

Protein fraction was extracted from berries at AR using the method previously described by Negri et al. 2008 [72] with some modifications. Thirteen berries per biological replicate (n=3) were peeled, and berry skins were finely powdered in liquid nitrogen using a pestle and mortar. Two grams of the powder were then resuspended in 10 mL of extraction buffer [0.7 M sucrose (Sigma-Aldrich Corp., St Louis, MO, USA), 0.5 M Tris-HCl pH 8 (MP Biomedicals, California, USA), 10 mM disodium EDTA salt (Promega, Madison, WI, USA), 1 mM PMSF (phenylmethylsulfonyl fluoride, Sigma-Aldrich Corp., St Louis, MO, USA), 0.2 % (v/v) β-mercaptoethanol (Sigma-Aldrich Corp., St Louis, MO, USA), protease inhibitor cocktail (Sigma-Aldrich Corp., St Louis, MO, USA) and PVPP (Sigma-Aldrich Corp., St Louis, MO, USA)] and shaking 10 min at 4°C. Proteins were extracted by the addition of an equal volume of ice-cold Tris-buffered phenol pH 8 (Sigma-Aldrich Corp., St Louis, MO, USA). The sample was shaken for 30 min at 4°C, incubated for 2 h at 4°C and finally centrifuged at 5000 g for 20 min at 4°C to separate the phases. Then, 9 mL of the upper phenol phase was collected, and the proteins were precipitated by the addition of 40 mL of ice-cold 0.1 M ammonium acetate in methanol. The sample was vortexed briefly and maintained at -20°C overnight. Precipitated proteins were recovered by centrifuging at 13000 g for 30 min at 4°C, then washed again with cold methanolic ammonium acetate and three additional times with cold 80% (v/v) acetone. The final pellet was dried at room temperature and resuspended in 500 μL of buffer [7 M urea (Promega, Madison, WI, USA), 2 M thiourea (Sigma-Aldrich Corp., St Louis, MO, USA), 4% (v/v) IGEPAL (Sigma-Aldrich Corp., St Louis, MO, USA) and 50 mg mL<sup>-1</sup> DTT (Sigma-Aldrich Corp., St Louis, MO, USA)]. Finally, the sample was centrifuged at 13000 g for 3 min and the supernatant stored at -80°C until it was used for protein analysis. The protein concentration was determined by the Bradford assay (Bio-Rad Laboratories Inc, California, USA).

##### 4.6.2. Nano-LC-Orbitrap Tandem Mass Spectrometry (nano-LC-MS/MS) Protein Analysis

Fifty μg of total protein was boiled (95°C, 5 min) in Laemmli buffer [0.0625 M Tris base (Promega, Madison, WI, USA), 0.07 M Sodium Dodecyl Sulfate (SDS, Promega, Madison, WI, USA), 10% (v/v) glycerol (Promega, Madison, WI, USA), 5% β-mercaptoethanol (Sigma-Aldrich Corp., St Louis, MO, USA), 0.005% bromophenol blue (Sigma-Aldrich Corp., St Louis, MO, USA)] and run in 10% SDS-PAGE. The proteins were allowed to run only 2 cm into the separating gel. The gel was stained according to colloidal Coomassie Brilliant Blue G-250 (Sigma-Aldrich Corp., St Louis, MO, USA) procedure [73], and the dried fragments of the gel corresponding to each biological replicate were sent to the Proteomics Core Facility CEQUIBIEM, Buenos Aires, Argentina. Proteins were reduced with 10 mM DTT for 45 min at 56°C and alkylated with 50 mM iodoacetamide (Sigma-Aldrich Corp., St Louis, MO, USA) for 45 min in darkness. Proteins were digested overnight with sequencing-grade modified trypsin (Promega, Madison, WI, USA). Then, the samples were lyophilized and resuspended with 30 μL of 0.1% trifluoroacetic acid (Sigma-Aldrich Corp., St Louis,

MO, USA). Zip-Tip C18 (Merck Millipore, Burlington, MA, USA) columns were used for desalting. Resulted peptides were separated in a nano-HPLC (EASY-nLC 1000, Thermo Fisher Scientific, Germany) coupled to a mass spectrometer with Orbitrap technology (Q-Exactive with High Collision Dissociation cell and Orbitrap analyzer, Thermo Fisher Scientific, Germany). Peptides were ionized by electrospray (EASY-SPRAY, ThermoScientific, Germany) at a voltage of 1.5 to 3.5 kV.

#### 4.7. Proteomics Data Analysis

Proteome Discoverer 2.2 software (ThermoScientific, Germany) was used to match the identity of peptides to the grapevine reference proteome set from uniprot (*Vitis vinifera*- UP000009183-Uniprot). The raw intensity values obtained from the MS data were normalized using the total ion current normalization method. The critical search parameters were as follows: precursor ion mass tolerance of 10 ppm, fragment mass tolerance of 0.05 Da, trypsin enzyme with a maximum of two missed cleavages allowed, variable modifications including oxidation and carbamidomethylation of cysteine, and a minimum of two peptides identified per protein. Missing values in the dataset were calculated by the principal component method using the package *missMDA* in R. Only proteins with high confidence and a percolator  $q$ -value lower than 0.01 were considered for the one-way ANOVA analysis.

#### 4.8. Statistical and Bioinformatic Analysis

Data were analyzed using software platform R 4.1.1. A multi-factor ANOVA was used to evaluate effects of ABA, GA<sub>3</sub>, developmental stage and their interactions on BFW, TSS, berry total polyphenols, berry total anthocyanins, and berry H<sub>2</sub>O<sub>2</sub> content kinetics using the *aov* function. For the analysis of Log<sub>2</sub> Fold-Change, berry anthocyanins and non-anthocyanins profile and MDA relative amount, one-way ANOVA followed by Fisher's least significant difference (LSD) test was applied, using *aov* function. Principal component analysis (PCA) was performed using the function *prcomp* from the *factoextra* package in R. The effects of TSS and H<sub>2</sub>O<sub>2</sub> content on berry total anthocyanins accumulation across three developmental stages were investigated by a linear mixed-effects model. "Treatments" was considered as a random effect on the intercept and slopes, meanwhile "TSS" and "H<sub>2</sub>O<sub>2</sub>" were considered as fixed effects. The linear mixed-effects regression was fitted using the function *lmer* from the *lme4* R package. The  $p$ -values of the fixed effects were obtained with the function *anova* from *lmerTest* package in R. Total variance explained by the model was partitioned with the function *r.squaredGLMM* from the *MuMIn* R package, in order to estimate the fraction of variance explained by the fixed and random effects. To identify differentially abundant proteins (DAPs), one-way ANOVA was performed with a significance threshold of  $p < 0.05$  and  $q < 0.05$  (for multiple comparisons), using *aov* function and *qvalue* package. The heatmaps used for treatment comparison were designed using the *heatmap* package. Bubble plots showing GO terms were designed using the *ggplot2* package and custom R scripts. Selected GO terms for biological processes were retrieved from STRING functional enrichment of stringApp 2.0.3 [74] in the Cytoscape 3.10.1 open software platform [75] with the grapevine reference genome as background and avoiding redundancy. The main network of each cluster, from the  $k$ -means clustering heatmap, was re-clustered with the MCL algorithm in stringApp for Cytoscape, with an inflation value of 4. In this sense, each heatmap cluster was labeled with their most representative GO term for biological function, which was retrieved by setting the redundancy cutoff to 0 in STRING functional enrichment.

## 5. Conclusions

For our knowledge, this is the first report showing that ABA and GA<sub>3</sub> modify the H<sub>2</sub>O<sub>2</sub> levels during grapevine berry ripening. We demonstrated how these hormones modulate the dynamics of berry total anthocyanins by regulating TSS and H<sub>2</sub>O<sub>2</sub> levels across each stage of berry development (OOR, AR and FR). The diminished H<sub>2</sub>O<sub>2</sub> levels in ABA- and GA<sub>3</sub>-treated berries at AR were attributed to both elevated levels of ROS-scavenging and oxidative stress response proteins, as well

as decreased levels of ROS-generating proteins. Furthermore, the increased accumulation of E-viniferin and quercetin in ABA and GA<sub>3</sub>-treated berries likely strengthened H<sub>2</sub>O<sub>2</sub> scavenging activity. However, further investigations are necessary to uncover the molecular mechanisms underlying ROS generation in ABA and GA<sub>3</sub>-treated berries during ripening. These findings contribute significantly to our comprehension of the ABA and GA<sub>3</sub> impact on berry ripening in wine cultivars, particularly in Malbec grapevines.

**Supplementary Materials:** The following supporting information can be downloaded at: www.mdpi.com/xxx/s1, Supplementary Figure S1: Enrichment analysis of berry skins differentially abundant proteins (DAPs) at almost ripe stage (AR); Supplementary Figure S2: Anthocyanins biosynthesis pathway; Supplementary Figure S3: Relative malondialdehyde (MDA) amount in berry skins at almost ripe stage (AR); Supplementary Table S1: Proteins differentially abundant in berry skins at almost ripe stage (AR); Supplementary Table S2: Anthocyanins predictive model using a linear mixed-effects regression.

**Author Contributions:** G.M. and R.A. conducted the experiment and carried out the physiological and biochemical analysis. G.M. carried out statistical and bioinformatic analysis. F.B., L.B. and M.P. carried out biochemical analysis. L.A. and A.F. participated in HPLC-MWD analysis. P.P. collaborated in experiment design, decided strategies and funding acquisition. J.J.C. provided insightful suggestions. G.M. wrote the body of the paper. All authors have read and agreed to the published version of the manuscript.

**Funding:** This work was supported by ANPCyT (Grant number: BID PICT 2016-2668) and CONICET (PIP 11220200100688CO). L.B. and L.A. have a CONICET scholarship; G.M., R.A., F.B., A.F., J.J.C. and P.P. are fellows of CONICET; M.P. is a fellow of INTA.

**Acknowledgments:** Special thanks to Fernando Buscema from Catena Institute of Wine for generously providing the experimental site at La Pirámide vineyard for our experiments.

**Conflicts of Interest:** The authors declare no conflicts of interest.

## References

1. Delrot S, Conde C. Biochemical Changes throughout Grape Berry Development and Fruit and Wine Quality. *Food*. 2007 Jan 1;1(1):1–22.
2. Fanzone M, Zamora F, Jofré V, Assof M, Gómez-Cordovés C, Peña-Neira Á. Phenolic characterisation of red wines from different grape varieties cultivated in Mendoza province (Argentina). *J Sci Food Agric*. 2012 Feb;92(3):704–18.
3. Downey MO, Dokoozlian NK, Krstic MP. Cultural Practice and Environmental Impacts on the Flavonoid Composition of Grapes and Wine: A Review of Recent Research. *Am J Enol Vitic*. 2006 Sep;57(3):257–68.
4. McAtee P, Karim S, Schaffer RJ, David K. A dynamic interplay between phytohormones is required for fruit development, maturation, and ripening. *Front Plant Sci*. 2013 Apr 17;4(79):1–7.
5. Wheeler S, Loveys B, Ford C, Davies C. The relationship between the expression of abscisic acid biosynthesis genes, accumulation of abscisic acid and the promotion of *Vitis vinifera* L. berry ripening by abscisic acid. *Aust J Grape Wine Res*. 2009;15(3):195–204.
6. Gambetta GA, Matthews MA, Shaghasi TH, McElrone AJ, Castellarin SD. Sugar and abscisic acid signaling orthologs are activated at the onset of ripening in grape. *Planta*. 2010 Jun;232(1):219–34.
7. Bennett J, Meiyalaghan S, Nguyen HM, Boldingh H, Cooney J, Elborough C, et al. Exogenous abscisic acid and sugar induce a cascade of ripening events associated with anthocyanin accumulation in cultured Pinot Noir grape berries. *Front Plant Sci*. 2023 Dec 21;14:1–15.
8. Murcia G, Pontin M, Reinoso H, Baraldi R, Bertazza G, Gómez-Talquencia S, et al. ABA and GA<sub>3</sub> increase carbon allocation in different organs of grapevine plants by inducing accumulation of non-structural carbohydrates in leaves, enhancement of phloem area and expression of sugar transporters. *Physiol Plant*. 2016 Mar 1;156(3):323–37.
9. Ferrara G, Mazzeo A, Matarrese AMS, Pacucci C, Pacifico A, Gambacorta G, et al. Application of Abscisic Acid (S-ABA) to ‘Crimson Seedless’ Grape Berries in a Mediterranean Climate: Effects on Color, Chemical Characteristics, Metabolic Profile, and S-ABA Concentration. *J Plant Growth Regul*. 2013 Sep 1;32(3):491–505.
10. Pilati S, Bagagli G, Sonago P, Moretto M, Brazzale D, Castorina G, et al. Abscisic Acid Is a Major Regulator of Grape Berry Ripening Onset: New Insights into ABA Signaling Network. *Front Plant Sci*. 2017 Jun 21;8:1093.
11. Li J, Liu B, Li X, Li D, Han J, Zhang Y, et al. Exogenous Abscisic Acid Mediates Berry Quality Improvement by Altered Endogenous Plant Hormones Level in “Ruiduhongyu” Grapevine. *Front Plant Sci*. 2021;12:1–19.

12. Murcia G, Pontin M, Piccoli P. Role of ABA and Gibberellin A3 on gene expression pattern of sugar transporters and invertases in *Vitis vinifera* cv. Malbec during berry ripening. *Plant Growth Regul.* 2018 Mar;84(2):275–83.
13. Pahi B, Rout CK, Saxena D. Effects of gibberellic acid (GA3) on quality and yield in grapes. *Int J Chem Stud.* 2020;8(6):2362–7.
14. Moreno D, Berli FJ, Piccoli PN, Bottini R. Gibberellins and Abscisic Acid Promote Carbon Allocation in Roots and Berries of Grapevines. *J Plant Growth Regul.* 2011 Jun 1;30(2):220–8.
15. Peppi MC, Fidelibus MW, Dokoozlian N. Abscisic Acid Application Timing and Concentration Affect Firmness, Pigmentation, and Color of 'Flame Seedless' Grapes. *HortScience.* 2006 Oct 1;41(6):1440–5.
16. Roberto SR, de Assis AM, Yamamoto LY, Miotto LCV, Sato AJ, Koyama R, et al. Application timing and concentration of abscisic acid improve color of 'Benitaka' table grape. *Sci Hort.* 2012 Jul 13;142:44–8.
17. Koyama R, Roberto SR, de Souza RT, Borges WFS, Anderson M, Waterhouse AL, et al. Exogenous Abscisic Acid Promotes Anthocyanin Biosynthesis and Increased Expression of Flavonoid Synthesis Genes in *Vitis vinifera* × *Vitis labrusca* Table Grapes in a Subtropical Region. *Front Plant Sci.* 2018 Mar 26;9:323.
18. Jimenez A, Creissen G, Kular B, Firmin J, Robinson S, Verhoeyen M, et al. Changes in oxidative processes and components of the antioxidant system during tomato fruit ripening. *Planta.* 2002 Mar 1;214(5):751–8.
19. Qin G, Meng X, Wang Q, Tian S. Oxidative damage of mitochondrial proteins contributes to fruit senescence: a redox proteomics analysis. *J Proteome Res.* 2009 May;8(5):2449–62.
20. Blokhina O, Virolainen E, Fagerstedt KV. Antioxidants, oxidative damage and oxygen deprivation stress: a review. *Ann Bot.* 2003 Jan;91 Spec No(2):179–94.
21. Mhamdi A, Van Breusegem F. Reactive oxygen species in plant development. *Dev Camb Engl.* 2018 Aug 9;145(15):dev164376.
22. Kärkönen A, Kuchitsu K. Reactive oxygen species in cell wall metabolism and development in plants. *Phytochemistry.* 2015 Apr 1;112:22–32.
23. Apel K, Hirt H. Reactive oxygen species: metabolism, oxidative stress, and signal transduction. *Annu Rev Plant Biol.* 2004;55:373–99.
24. Gechev TS, Van Breusegem F, Stone JM, Denev I, Laloi C. Reactive oxygen species as signals that modulate plant stress responses and programmed cell death. *BioEssays News Rev Mol Cell Dev Biol.* 2006 Nov;28(11):1091–101.
25. Huang H, Ullah F, Zhou DX, Yi M, Zhao Y. Mechanisms of ROS Regulation of Plant Development and Stress Responses. *Front Plant Sci.* 2019 Jun 25;10:800.
26. Pilati S, Perazzolli M, Malossini A, Cestaro A, Demattè L, Fontana P, et al. Genome-wide transcriptional analysis of grapevine berry ripening reveals a set of genes similarly modulated during three seasons and the occurrence of an oxidative burst at véraison. *BMC Genomics.* 2007 Nov 22;8(1):428.
27. Pilati S, Brazzale D, Guella G, Milli A, Ruberti C, Biasioli F, et al. The onset of grapevine berry ripening is characterized by ROS accumulation and lipoxygenase-mediated membrane peroxidation in the skin. *BMC Plant Biol.* 2014 Apr 2;14(1):87.
28. Kumar V, Irfan M, Ghosh S, Chakraborty N, Chakraborty S, Datta A. Fruit ripening mutants reveal cell metabolism and redox state during ripening. *Protoplasma.* 2016 Mar 1;253(2):581–94.
29. Brennan T, Frenkel C. Involvement of Hydrogen Peroxide in the Regulation of Senescence in Pear 1. *Plant Physiol.* 1977 Mar;59(3):411–6.
30. Huan C, Jiang L, An X, Yu M, Xu Y, Ma R, et al. Potential role of reactive oxygen species and antioxidant genes in the regulation of peach fruit development and ripening. *Plant Physiol Biochem.* 2016 Jul 1;104:294–303.
31. Guo D L, Wang Z g., Li Q, Gu S c., Zhang G h., Yu Y h. Hydrogen peroxide treatment promotes early ripening of Kyoho grape. *Aust J Grape Wine Res.* 2019;25(3):357–62.
32. Guo DL, Wang ZG, Pei MS, Guo LL, Yu YH. Transcriptome analysis reveals mechanism of early ripening in Kyoho grape with hydrogen peroxide treatment. *BMC Genomics.* 2020 Nov 11;21:784.
33. Xu L, Yue Q, Xiang G, Bian F, Yao Y. Melatonin promotes ripening of grape berry via increasing the levels of ABA, H<sub>2</sub>O<sub>2</sub>, and particularly ethylene. *Hortic Res.* 2018 Aug 1;5(1):1–11.
34. Sun H, Cao X, Wang X, Zhang W, Li W, Wang X, et al. RBOH-dependent hydrogen peroxide signaling mediates melatonin-induced anthocyanin biosynthesis in red pear fruit. *Plant Sci.* 2021 Dec 1;313:111093.
35. Wen B, Zhang F, Wu X, Li H. Characterization of the Tomato (*Solanum lycopersicum*) Pectin Methyltransferases: Evolution, Activity of Isoforms and Expression During Fruit Ripening. *Front Plant Sci.* 2020 Mar 3;11:1–17.
36. Wang D, Yeats TH, Uluisik S, Rose JKC, Seymour GB. Fruit Softening: Revisiting the Role of Pectin. *Trends Plant Sci.* 2018 Apr 1;23(4):302–10.
37. Berli FJ, Alonso R, Beltrano J, Bottini R. High-Altitude Solar UV-B and Abscisic Acid Sprays Increase Grape Berry Antioxidant Capacity. *Am J Enol Vitic.* 2015 Feb;66(1):65–72.

38. Berli FJ, Fanzone M, Piccoli P, Bottini R. Solar UV-B and ABA are involved in phenol metabolism of *Vitis vinifera* L. increasing biosynthesis of berry skin polyphenols. *J Agric Food Chem*. 2011 May 11;59(9):4874–84.
39. Koyama K, Sadamatsu K, Goto-Yamamoto N. Abscisic acid stimulated ripening and gene expression in berry skins of the Cabernet Sauvignon grape. *Funct Integr Genomics*. 2010 Aug;10(3):367–81.
40. Giribaldi M, Gény L, Delrot S, Schubert A. Proteomic analysis of the effects of ABA treatments on ripening *Vitis vinifera* berries. *J Exp Bot*. 2010 May 1;61(9):2447–58.
41. Yang L, Zhang J, He J, Qin Y, Hua D, Duan Y, et al. ABA-Mediated ROS in Mitochondria Regulate Root Meristem Activity by Controlling PLETHORA Expression in Arabidopsis. Yu H, editor. *PLoS Genet*. 2014 Dec 18;10(12):e1004791.
42. Jiang M, Zhang J. Effect of Abscisic Acid on Active Oxygen Species, Antioxidative Defence System and Oxidative Damage in Leaves of Maize Seedlings. *Plant Cell Physiol*. 2001 Nov 15;42(11):1265–73.
43. Ye N, Zhu G, Liu Y, Li Y, Zhang J. ABA controls H<sub>2</sub>O<sub>2</sub> accumulation through the induction of OsCATB in rice leaves under water stress. *Plant Cell Physiol*. 2011 Apr;52(4):689–98.
44. Shah SH, Islam S, Mohammad F, Siddiqui MH. Gibberellic Acid: A Versatile Regulator of Plant Growth, Development and Stress Responses. *J Plant Growth Regul*. 2023 Jun 6; 42(12):7352-7373.
45. Hung KT, Cheng DG, Hsu YT, Kao CH. Abscisic acid-induced hydrogen peroxide is required for anthocyanin accumulation in leaves of rice seedlings. *J Plant Physiol*. 2008 Aug 25;165(12):1280–7.
46. Loreti E, Povero G, Novi G, Solfanelli C, Alpi A, Perata P. Gibberellins, jasmonate and abscisic acid modulate the sucrose-induced expression of anthocyanin biosynthetic genes in Arabidopsis. *New Phytol*. 2008;179(4):1004–16.
47. An JP, Xu RR, Wang XN, Zhang XW, You CX, Han Y. MdbHLH162 connects the gibberellin and jasmonic acid signals to regulate anthocyanin biosynthesis in apple. *J Integr Plant Biol*. 2024;66(2):265–84.
48. Berli FJ, Moreno D, Piccoli P, Hespagnol-Viana L, Silva MF, Bressan-Smith R, et al. Abscisic acid is involved in the response of grape (*Vitis vinifera* L.) cv. Malbec leaf tissues to ultraviolet-B radiation by enhancing ultraviolet-absorbing compounds, antioxidant enzymes and membrane sterols. *Plant Cell Environ*. 2010 Dec; 33(1):1-10.
49. Pontin M, Murcia G, Bottini R, Fontana A, Bolcato L, Piccoli P. Nitric oxide and abscisic acid regulate osmoprotective and antioxidative mechanisms related to water stress tolerance of grapevines. *Aust J Grape Wine Res*. 2021;27(3):392–405.
50. Jiang Z, Zhu H, Zhu H, Tao Y, Liu C, Liu J, et al. Exogenous ABA Enhances the Antioxidant Defense System of Maize by Regulating the AsA-GSH Cycle under Drought Stress. *Sustainability*. 2022 Jan;14(5):3071.
51. Fu J, Li L, Wang S, Yu N, Shan H, Shi Z, et al. Effect of gibberellic acid on photosynthesis and oxidative stress response in maize under weak light conditions. *Front Plant Sci*. 2023 Feb 16;14:1–13.
52. Yang L, Luo S, Jiao J, Yan W, Zeng B, He H, et al. Integrated Transcriptomic and Metabolomic Analysis Reveals the Mechanism of Gibberellic Acid Regulates the Growth and Flavonoid Synthesis in *Phellodendron chinense* Schneid Seedlings. *Int J Mol Sci*. 2023 Nov 7;24(22):16045.
53. ul Haq S, Khan A, Ali M, Khattak AM, Gai WX, Zhang HX, et al. Heat Shock Proteins: Dynamic Biomolecules to Counter Plant Biotic and Abiotic Stresses. *Int J Mol Sci*. 2019 Oct 25;20(21):5321.
54. Santos CVD, Rey P. Plant thioredoxins are key actors in the oxidative stress response. *Trends Plant Sci*. 2006 Jul 1;11(7):329–34.
55. Sevilla F, Martí MC, De Brasi-Velasco S, Jiménez A. Redox regulation, thioredoxins, and glutaredoxins in retrograde signalling and gene transcription. *J Exp Bot*. 2023 Oct 13;74(19):5955–69.
56. Gullner G, Komives T, Király L, Schröder P. Glutathione S-Transferase Enzymes in Plant-Pathogen Interactions. *Front Plant Sci*. 2018 Dec 21;9:1–19.
57. Sun L, Fan X, Zhang Y, Jiang J, Sun H, Liu C. Transcriptome analysis of genes involved in anthocyanins biosynthesis and transport in berries of black and white spine grapes (*Vitis davidii*). *Hereditas*. 2016 Dec 7;153(1):17.
58. Kussmaul L, Hirst J. The mechanism of superoxide production by NADH:ubiquinone oxidoreductase (complex I) from bovine heart mitochondria. *Proc Natl Acad Sci*. 2006 May 16;103(20):7607–12.
59. Singh P, Arif Y, Miszczuk E, Bajguz A, Hayat S. Specific Roles of Lipxygenases in Development and Responses to Stress in Plants. *Plants*. 2022 Apr 4;11(7):979.
60. Xi FF, Guo LL, Yu YH, Wang Y, Li Q, Zhao HL, et al. Comparison of reactive oxygen species metabolism during grape berry development between ‘Kyoho’ and its early ripening bud mutant ‘Fengzao.’ *Plant Physiol Biochem*. 2017 Sep 1;118:634–42.
61. Dominguez PG, Frankel N, Mazuch J, Balbo I, Iusem N, Fernie AR, et al. ASR1 Mediates Glucose-Hormone Cross Talk by Affecting Sugar Trafficking in Tobacco Plants. *Plant Physiol*. 2013 Mar 1;161(3):1486–500.
62. Çakir B, Agasse A, Gaillard C, Saumonneau A, Delrot S, Atanassova R. A Grape ASR Protein Involved in Sugar and Abscisic Acid Signaling. *Plant Cell*. 2003 Sep 2;15(9):2165–80.

63. Nopo-Olazabal C, Hubstenberger J, Nopo-Olazabal L, Medina-Bolivar F. Antioxidant Activity of Selected Stilbenoids and Their Bioproduction in Hairy Root Cultures of Muscadine Grape (*Vitis rotundifolia* Michx.). *J Agric Food Chem*. 2013 Dec 4;61(48):11744–58.
64. Singh P, Arif Y, Bajguz A, Hayat S. The role of quercetin in plants. *Plant Physiol Biochem*. 2021 Sep 1;166:10–9.
65. Coombe BG. Growth Stages of the Grapevine: Adoption of a system for identifying grapevine growth stages. *Aust J Grape Wine Res*. 1995;1(2):104–10.
66. Berli F, D'Angelo J, Cavagnaro B, Bottini R, Wuilloud R, Silva MF. Phenolic composition in grape (*Vitis vinifera* L. cv. Malbec) ripened with different solar UV-B radiation levels by capillary zone electrophoresis. *J Agric Food Chem*. 2008 May 14;56(9):2892–8.
67. Urvieta R, Buscema F, Bottini R, Coste B, Fontana A. Phenolic and sensory profiles discriminate geographical indications for Malbec wines from different regions of Mendoza, Argentina. *Food Chem*. 2018 Nov 1;265:120–7.
68. Antonioli A, Fontana AR, Piccoli P, Bottini R. Characterization of polyphenols and evaluation of antioxidant capacity in grape pomace of the cv. Malbec. *Food Chem*. 2015 Jul 1;178:172–8.
69. Ferreyra S, Torres-Palazzolo C, Bottini R, Camargo A, Fontana A. Assessment of in-vitro bioaccessibility and antioxidant capacity of phenolic compounds extracts recovered from grapevine bunch stem and cane by-products. *Food Chem*. 2021 Jun 30;348:129063.
70. Junglee S, Urban L, Sallanon H, Lopez-Lauri F. Optimized Assay for Hydrogen Peroxide Determination in Plant Tissue Using Potassium Iodide. *Am J Anal Chem*. 2014;05(11):730–6.
71. Beligni MV, Lamattina L. Nitric oxide interferes with plant photo-oxidative stress by detoxifying reactive oxygen species. *Plant Cell Environ*. 2002;25(6):737–48.
72. Negri AS, Prinsi B, Rossoni M, Failla O, Scienza A, Cocucci M, et al. Proteome changes in the skin of the grape cultivar Barbera among different stages of ripening. *BMC Genomics*. 2008 Aug 8;9(1):378.
73. Neuhoff V, Arold N, Taube D, Ehrhardt W. Improved staining of proteins in polyacrylamide gels including isoelectric focusing gels with clear background at nanogram sensitivity using Coomassie Brilliant Blue G-250 and R-250. *Electrophoresis*. 1988 Jun;9(6):255–62.
74. Doncheva NT, Morris JH, Gorodkin J, Jensen LJ. Cytoscape StringApp: Network Analysis and Visualization of Proteomics Data. *J Proteome Res*. 2019 Feb 1;18(2):623–32.
75. Shannon P, Markiel A, Ozier O, Baliga NS, Wang JT, Ramage D, et al. Cytoscape: a software environment for integrated models of biomolecular interaction networks. *Genome Res*. 2003 Nov;13(11):2498–504.

**Disclaimer/Publisher's Note:** The statements, opinions and data contained in all publications are solely those of the individual author(s) and contributor(s) and not of MDPI and/or the editor(s). MDPI and/or the editor(s) disclaim responsibility for any injury to people or property resulting from any ideas, methods, instructions or products referred to in the content.